Comptes Rendus
Géoscience — Sciences de la Planète
Supplementary material to the article available at:
https://doi.org/10.5802/crgeos.191

Supplementary material: Onset of a submarine eruption east of Mayotte, Comoros archipelago: the first ten months seismicity of the seismo-volcanic sequence (2018–2019)

Nicolas Mercury *, [a, b], **Anne Lemoine** [b], **Cécile Doubre** [a], **Didier Bertil** [b], **Jérôme Van Der Woerd** [a], **Roser Hoste-Colomer** [b] and **Jean Battaglia** [c]

[a] Institut Terre et Environnement de Strasbourg, CNRS UMR 7063, Université de Strasbourg, 5 rue René Descartes, 67084 Strasbourg Cedex, France

[b] BRGM, Department of Risks and Prevention, 3 av. Claude-Guillemin - BP 36009, 45060 Orléans Cedex 2, France

[c] Laboratoire Magmas et Volcans, UMR 6524 CNRS, UMR 163 IRD, Université Clermont Auvergne, 6 Av. Blaise Pascal, 63170 Aubière, France

E-mails: n.mercury@brgm.fr (N. Mercury), a.lemoine@brgm.fr (A. Lemoine), cecile.doubre@unistra.fr (C. Doubre), d.bertil@brgm.fr (D. Bertil), jerome.vanderwoerd@unistra.fr (J. Van Der Woerd), r.hostecolomer@brgm.fr (R. Hoste-Colomer), j.battaglia@opgc.univ-bpclermont.fr (J. Battaglia)

Seismic networks evolution along the Comoros archipelago (2015–2019)

Before 2015, the sparse and moderate regional seismicity is detected and localized only by international or regional survey networks [Bertil et al., 2021, Figure S1], with broadband stations in eastern Africa (Kenya, Mozambique) and nearby islands in the western Indian Ocean: Madagascar, La Réunion, Seychelles [see Bertil et al., 2021; Figure S2, Table 1]. The detection threshold for seismic events occurring within the Comoros archipelago is estimated to a moment magnitude of 4.3 [Bertil and François, 2016].

In 2017, the Grande Comore seismic network, monitoring the Karthala activity, benefits from the installation of its first four broadband seismic stations (KA.SBC, KA.CAB, KA.MOIN, KA.DEMB; Figure S2b). In Mayotte, the first strong motion seismic stations (YTMZ, MDZA and MILA) are fully operational in June 2016 [Resif, 1995]. YTMZ signals are transmitted in real time, while data recorded at MDZA and MILA are recovered every three to four months.

In May 2018, stations RA.YTMZ and RA.MILA have internal clock issues that are only fixed at the end of June 2018 and end of August 2018, respectively (Figure S2e–f). Thus, MDZA is the only reliable station on Mayotte (Figure S2c-f). At the end of June 2018, three additional stations are installed in Mayotte (Figure S2d–f): a medium band station

* Corresponding author.

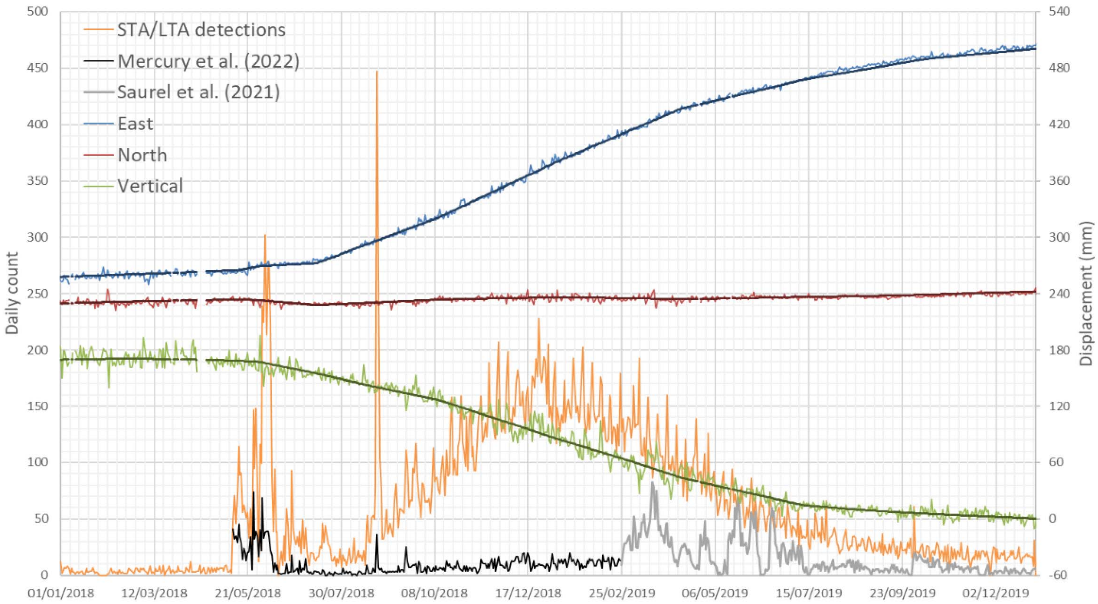

Supplementary Figure S1. Time evolution of the number of detections found by STA/LTA, on the vertical component of station YTMZ (orange line), from 1 January 2018 to 31 December 2019. GNSS displacements (along east, north, and vertical axis) from Lemoine et al. [2020a] are shown, as well as number of located events from this work (black line) and Saurel et al. [2022, grey line].

Supplementary Table S1. Network geometries tested for location reliability

Network distribution	Mayotte stations	GE.SBV data	Distant stations
N1	PMZI[a]	Yes	All stations > 500 km ($n = 6$)
N2	PMZI, YTMZ, MCHI, RAE55	Yes	All stations > 500 km ($n = 6$)
N3	PMZI, YTMZ, MCHI, RAE55, MILA	Yes	All stations > 500 km ($n = 6$)
N4	PMZI	No	All stations > 500 km ($n = 6$)
N5	PMZI, MCHI	No	All stations > 500 km ($n = 6$)
N6	PMZI, YTMZ, MCHI,	No	All stations > 500 km ($n = 6$)
N7	PMZI, YTMZ, MCHI, RAE55	No	All stations > 500 km ($n = 6$)
N8	PMZI, YTMZ, MCHI, RAE55, MILA	No	All stations > 500 km ($n = 6$)

[a] PMZI is the new station at the location of the MDZA station recording at the onset of the sequence.

MCHI (dedicated initially to educational purposes, Edusismo network https://www.sciencesalecole.org/plan-sismos-a-lecole-reseau/; Berenguer et al., 2020) on 18 June and two RaspberryShake stations on 25 June, a one vertical component AM.RAE55 and a 3-component AM.RCBF0 [Bes de Berc et al., 2019]. The latter one only records for 10 days. The installation of OBS above the seismic area at the end of February 2019 [Saurel et al., 2022], completed by four inland velocimeters in March 2019 (1T.PMZI, 1T.MTSB, QM.KNKL, QM.GGLO — QM is the Comoros Seismic Network; 1T is the temporary seismological network of Mayotte-, Figure S2) allows a better monitoring of the seismicity and active structures east of Mayotte [Feuillet et al., 2021, Foix et al., 2021; Lavayssière et al., 2022; Saurel et al., 2022].

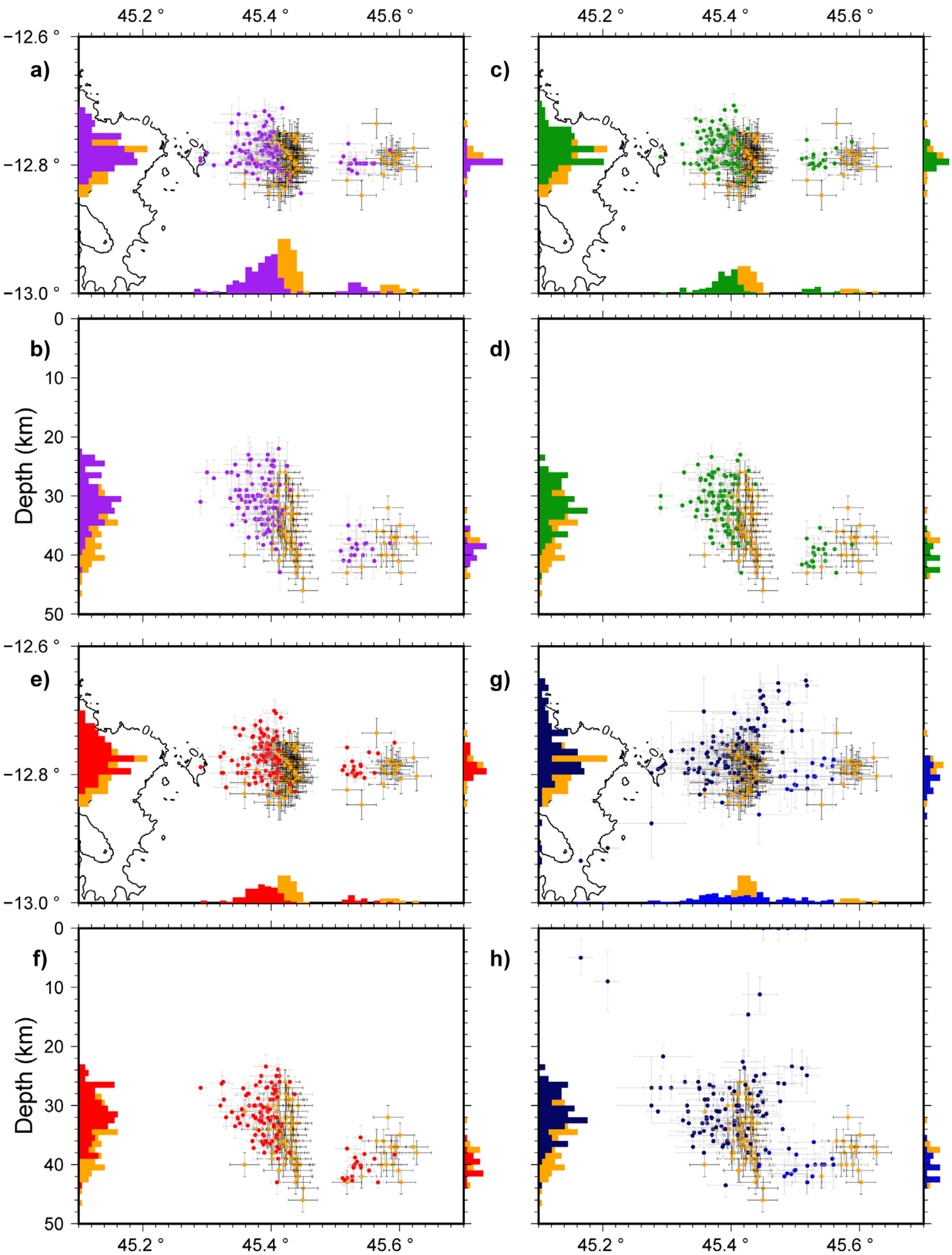

Supplementary Figure S2. Comparison of locations of a subset of 118 earthquakes between 2019 and 2020, using Saurel et al. [2022] events (orange dots) and our methodology of location for different distributions of the inland network (Table S1). Distribution in map view and vertical cross-section, for (a–b) N1 (purple), (c–d) N2 (green), (e–f) N3 (red), (g–h) N7 without station SBV (events in the proximal cluster are dark blue, others are light blue). Histogram distributions are shown for both clusters on the longitude axis, and for each cluster on the latitude and vertical axes (histogram of the proximal and distal clusters on the left and right, respectively).

Reliability of our monitoring network, compared to the later inland + OBS network accuracy

We ought to better determine the instrumental bias due to the initial network distributions (Figure S2), to improve the reliability of our locations. To do so, we present the comparison between locations using our velocity model and network distributions with locations of the same events using the latter OBS network along with more inland stations and an improved local velocity model from Saurel et al. [2022]. For the period from 25 February 2019 to 9 May 2020, Saurel et al. [2022] catalog uses the NonLinLoc location algorithm [Lomax et al., 2009] using a local hybrid 1D velocity model, deduced from 3 models: a P-wave velocity profile adapted from an active sonobuoy experiment [Coffin et al. [1986]; Jacques et al., 2019], a S-wave velocity profile calculated with receiver functions [Dofal et al., 2021] and the AK135 global velocity model [Kennett et al., 1995]. Due to the OBS distribution above the swarms and the denser inland seismic network, the horizontal and vertical uncertainties of 95% of the 5195 hypocentral locations are less than 5.0 km.

To compare the reliability of our locations, we selected events between March and December 2019, that have been as well located by Saurel et al. [2022], on which we had P and S pickings [Lemoine et al., 2020a; Bertil et al., 2021]. The selected events must have at least one P-wave arrival on the Karthala stations (CAB-SBC-MOIN-DEMB) and II.ABPO, along with both P and S phases on PMZI, SBV, MILA and either YTMZ or MCHI. This led us to work on a reduced set of 118 earthquakes recorded from 18 May to 21 December 2019 with magnitudes between 2.9 and 5.2, that have been as well located by Saurel et al. [2022].

In order to reproduce the limitations of the sparse seismic network and its evolution between 10 May 2018 and 24 February 2019 (Figure S2), we decipher the input arrival time database as described in the Table S1 and we follow the same procedure of location described in the main text of the paper (Section 3.2).

For the first three seismic network configurations that include SBV (N1, N2, N3), we note that the seismic pattern is well reproduced, both clusters are well separated, with a no-event zone between 45.6 °E and 45.8 °E (Figure S2a–c). All the earthquakes with any of those three degraded configurations are located in the same cluster as in Saurel et al. [2022] catalog. The proximal cluster is shifted to the west, north and up, by approximately 4.1 km, 1.7 km, and 3.8 km, respectively (Figure S2a–f). The distal cluster is shifted to the west and down, by 5.5 km and 1.3 km, respectively (Figure S2a–f). 95% of uncertainties calculated with HYPO71 and the regional velocity model are below 3 km and 4 km for N1, 2 km and 2 km for N2 and N3, along the horizontal and vertical components, respectively.

As for the locations without SBV, we tested the N7 configuration. The two clusters are no longer explicitly distinct with a vertical separation (Figure S2d). Instead, the two clusters are distributed on two parallel ENE-WSW elongated swarms. Similarly, at depth, the clusters are separated in two deep-west to closer-to-the-surface-east sub-parallel swarms. On the proximal cluster, locations of N7 are scattered and shifted to the west, north and up, by 3.0 km, 3.0 km, and 5.8 km, respectively, compared to locations in Saurel et al. [2022] catalog (Figure S1a). On the distal cluster, locations N7 are also scattered and shifted to the west, south and down, by 8.2 km, 1.5 km and 1.9 km, respectively, compared to locations in the Saurel et al. [2022] catalog (Figure S1a). 95% of uncertainties calculated with HYPO71, are below 6 km along the horizontal component and 3 km along the vertical component. We observe several locations dozens of kilometers away from the initial Saurel et al. [2022] locations. We also note several events mislocated close to the surface, between 0 and 15 km (Figure S2).

From this comparative study, we conclude that using inland stations only, including SBV station north of Madagascar, we get reliable locations, compared to a much more complete and well distributed seismic network. The lack of stations on top and close east of the seismic clusters tends to bring locations of events a few kilometers closer to Mayotte, with lower longitude values on both clusters and shallower earthquakes on the proximal one, the mean difference being above horizontal and vertical uncertainties given by Saurel et al. [2022].

However, locating earthquakes without the SBV station has several issues: the shape and separation of our two clusters is less accurate or even diffuse, and we get several events with locations distant dozens of kilometers from locations of Saurel et al. [2022]. Sensitivity of the network to its close east station absence is high, especially for small magnitudes with a low number of P and S phases earthquakes. Hence, we are more cautious while studying events located without SBV, between mid-June and mid-July 2018, and at the end of August (Figure S2e-f), associated with higher azimutal gaps.

We note that for the results of all the tests, the longitude difference is higher on the distal cluster, but as Saurel et al. [2022] mentioned, their location process was calibrated on proximal events mainly, so they believe that their distribution is less accurate on the distal cluster.

References

Berenguer, J.-L., Balestra, J., Jouffray, F., Mourau, F., Courboulex, F., and Virieux, J. (2020). Celebrating 25 years of seismology at schools in France. *Geosci. Commun.*, 3, 475–481.

Bes de Berc, M., Pestourie, R., Jund, H., and Broucke, C. (2019). A Complete Characterization of 27 OSOP Raspberryshakes Performed at EOST Seismic Instrumentation Facility. Poster X2.463, EGU2019-1660, EGU General Assembly.

Coffin, M. F., Rabinowitz, P. D., and Houtz, R. E. (1986). Crustal structure in the western Somali Basin. *Geophys. J. Int.*, 86(2), 331–369.

Kennett, B. L. N., Engdahl, E. R., and Buland, R. (1995). Constraints on seismic velocities in the Earth from traveltimes. *Geophys. J. Int.*, 122, 108–124.

Lomax, A., Michelini, A., Curtis, A., and Meyers, R. A. (2009). Earthquake location, direct, global-search methods. *Encycl. Complex. Syst. Sci.*, 5, 2449–2473.

Resif (1995). RESIF-RAP French Accelerometric Network. RESIF - Réseau Sismologique et géodésique Français. http://doi.org/10.15778/resif.ra.

Saurel, J. M., Jacques, E., Aiken, C., Lemoine, A., Retailleau, L., Lavayssière, A., Foix, O., Dofal, A., Laurent, A., Mercury, N., Crawford, W. C., Lemarchand, A., Daniel, R., Pelleau, P., Bès de Berc, M., Dectot, G., Bertil, D., Roullé, A., Broucke, C., Colombain, A., Jund, H., Besançon, S., Guyavarch, P., Kowalski, P., Roudaut, M., Apprioual, R., Battaglia, J., Bodihar, S., Boissier, P., Bouin, M. P., Brunet, C., Canjamalé, K., Catherine, P., Desfete, N., Doubre, C., Dretzen, R., Dumouch, T., Fernagu, P., Ferrazzini, V., Fontaine, F., Gaillot, A., Géli, L., Griot, C., Grunberg, M., Can Guzel, E., Hoste-Colomer, R., Lambotte, S., Lauret, F., Léger, F., Maros, E., Peltier, A., Vergne, J., Satriano, C., Tronel, F., Van der Woerd, J., Feuillet, N., Fouquet, Y., Jorry, S. J., Rinnert, E., and Thinon, I. (2022). "2019-02-25 to 2020-05-10 Mayotte eruption earthquake catalog relocated with OBS". https://doi.org/10.18715/IPGP.2021.kq136bzh, IPGP Research Collection, V1.